

Synthesis, crystal structures and magnetic properties of salts containing bis[hydrotris(3,5-dimethyl-1-pyrazolyl)borate]iron(III)

Susan J. Mason^a, Christopher M. Hill^a, Vince J. Murphy^a, Dermot O'Hare^{a,*},
David J. Watkin^b

^a *Inorganic Chemistry Laboratory, South Parks Road Oxford OX1 3QR, UK*

^b *Chemical Crystallography Laboratory, 9 Parks Road, Oxford OX1 3PD, UK*

Received 8 April 1994

Abstract

The salts $[\text{Fe}(\text{C}_{15}\text{H}_{22}\text{N}_6\text{B})_2][\text{PF}_6]$, $[\text{Fe}(\text{C}_{15}\text{H}_{22}\text{N}_6\text{B})_2][\text{TCNQ}]\cdot\text{THF}$ and $[\text{Fe}(\text{C}_{15}\text{H}_{22}\text{N}_6\text{B})_2][\text{FeBr}_4]$ have been prepared and the first two subjected to X-ray diffraction studies. In $[\text{Fe}(\text{C}_{15}\text{H}_{22}\text{N}_6\text{B})_2][\text{PF}_6]$ the coordination geometry around the Fe centre is almost perfectly octahedral, with the Fe–N bond distances in the range 1.960(3)–1.970(3) Å, which are typical distances for low spin iron(III) complexes. In $[\text{Fe}(\text{C}_{15}\text{H}_{22}\text{N}_6\text{B})_2][\text{TCNQ}]\cdot\text{THF}$ the Fe–N bond lengths lie in the range 1.980(3)–1.949(2) Å, and there is essentially octahedral symmetry around the metal centre. In the case of $[\text{Fe}(\text{C}_{15}\text{H}_{22}\text{N}_6\text{B})_2][\text{TCNQ}]\cdot\text{THF}$ the $[\text{TCNQ}]^-$ anions lie in rows perpendicular to the crystallographic *bc*-plane, these rows being separated by parallel rows of $[\text{Fe}(\text{C}_{15}\text{H}_{22}\text{N}_6\text{B})_2]^+$ cations. The solid state magnetic susceptibility data for these compounds obey the Curie law ($\chi_M = C/T$) in the temperature range 6–300 K with $\mu_{\text{eff}} = 1.65, 2.55$ and $5.39 \mu_B$ for the three complexes respectively. None of these salts showed any evidence of short-range spin-spin interactions at low temperature.

Keywords: Iron; Crystal structure; Magnetic susceptibility; Pyrazolylborate; Charge-transfer; TCNQ

1. Introduction

The synthesis and characterisation of molecular inorganic solids that exhibit cooperative magnetic interactions is currently of great interest. For example, the metallocenium solids $[\text{M}(\eta\text{-C}_5\text{Me}_5)_2]^+[\text{TCNE}]^-$ (TCNE = tetracyanoethylene; M=Cr, Fe and Mn) exhibit ferromagnetically ordered ground states with Curie temperatures (T_c) of 3.65, 4.8 and 8.8 K respectively [1–3].

The electronic properties of the poly(1-pyrazolyl)borate ligand, which is a $6e^-$ donor, are often likened to those of the C_5H_5^- and C_5Me_5^- ligands, since it has been shown to form a large number of analogous complexes with similar reactivities. In addition this ligand system has been observed to have a greater stabilising influence upon the coordinated metal centre [4], often resulting in air-stable compounds [5]. For example, bis[hydrotris(3,5-dimethyl-1-pyrazolyl)

borate] complexes of manganese(II), copper(II) and zinc(II) were amongst those first synthesised by Trofimenco [6] in 1967. Interestingly bis(hydrotris(3,5-dimethyl-1-pyrazolyl)borate]iron(II) was found to undergo a high spin-low spin crossover between 150 and 250 K [7,8].

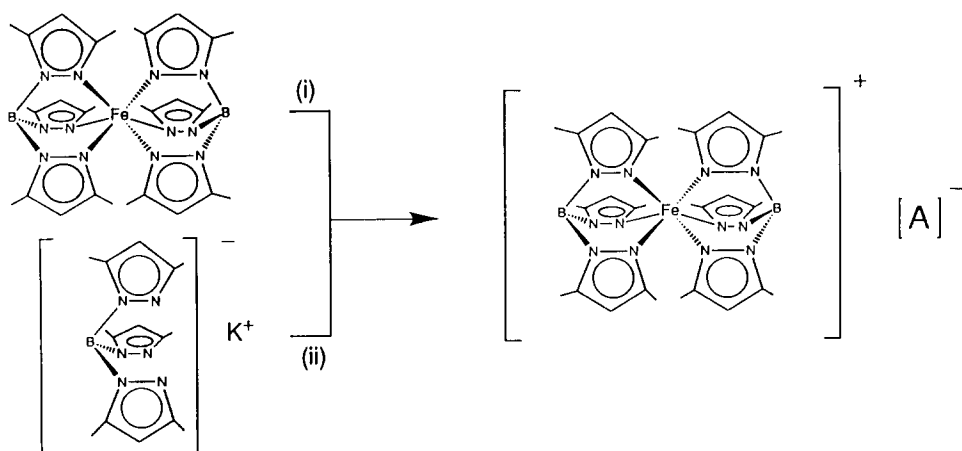
As part of our continuing interest in the magnetic properties of molecular materials we have been synthesising new inorganic salts containing bis[hydrotris(3,5-dimethyl-1-pyrazolyl)borate metal cations to investigate their potentially interesting solid state magnetic properties. Here we report the synthesis, crystal structures and magnetic properties of salts containing bis[hydrotris(3,5-dimethyl-1-pyrazolyl)borate]iron(III).

2. Experimental details

2.1. General

Solid state magnetic susceptibility measurements were recorded on microcrystalline samples using a

* Corresponding author.



Scheme 1. (i) For **1** $[\text{Fe}(\text{Cp})_2][\text{PF}_6]$ in CH_2Cl_2 at rt, 60%; For **2** TCNQ in CH_2Cl_2 at rt, 52%; For **3**. (ii) FeBr_3 in CH_2Cl_2 at rt, 52%.

Cryogenics Consultants SCU500 superconducting quantum interference device (SQUID) susceptometer, from 6–300 K. The susceptibilities were corrected for

the intrinsic diamagnetism of the sample container and the diamagnetism of the electronic cores of the constituent atoms. Infrared spectra were measured on a

Table 1
Crystallographic parameters for **1** and **2**

Compound formula	$\text{C}_{30}\text{H}_{44}\text{B}_2\text{F}_6\text{FeN}_{12}\text{P}$ (1)	$\text{C}_{46}\text{H}_{52}\text{B}_2\text{FeN}_{16}\text{O}$ (2)
Formula weight	794.85	926.17
Crystal system	monoclinic	triclinic
Space group	$P2_1/a$	$P\bar{1}$
$a/\text{\AA}$	12.747(2)	8.690(8)
$b/\text{\AA}$	13.737(2)	11.015(5)
$c/\text{\AA}$	10.431(1)	14.093(5)
$\alpha/^\circ$	90	114.66(4)
$\beta/^\circ$	93.69(1)	92.83(9)
$\gamma/^\circ$	90	98.04(7)
$V/\text{\AA}^3$	1823	1205
Z	2	1
D_c/gcm^{-3}	1.449	1.173
$F(000)$	826	440
Linear abs. coef./ cm^{-1}	43.717	3.574
Refinement		
Number of parameters	238	382
Ratio of data to parameters	10.57	7.86
Weighting scheme	Chebyshev (6.6, 2.0, 4.7)	Chebyshev (5.4, 3.3, 1.8)
Final R^a	0.0771	0.0571
Final R_w^b	0.0863	0.0682
Absorption correction		
Type	DIFABS	DIFABS
Min/max correction in θ	0.58/1.86	1.00/1.47
Data collection		
X-radiation	$\text{Cu K}\alpha$, $\lambda = 1.54180 \text{\AA}$	$\text{Mo K}\alpha$, $\lambda = 0.71069 \text{\AA}$
$\theta_{\text{min}}, \theta_{\text{max}}/^\circ$	0, 72	0, 24
ω -scan width parameters	$0.60 + 0.15 \tan \theta$	$1.10 + 0.35 \tan \theta$
Min/max h,k,l	-15/15 -1/16 -1/12	-1/9 -12/12 -16/16
Total data collected	4719	3805
Total unique data	3543	3757
Total observed data ($I > 3\sigma$)	2515	3002
Sheldrick merging R -factors	0.062	0.039

^a $R = \sum \|F_o\| - |F_c| / \sum |F_o|$;

^b $R_w = (\sum (|F_o| - |F_c|)^2 / \sum |F_o|^2)^{1/2}$

Perkin-Elmer 1700FT spectrometer between KBr plates. Elemental microanalyses were performed by the Analytical Services of the Inorganic Chemistry Laboratory. $[\text{Fe}(\text{C}_{15}\text{H}_{22}\text{N}_6\text{B})_2]$ was prepared by literature methods [6].

2.2. Synthesis of $[\text{Fe}(\text{C}_{15}\text{H}_{22}\text{N}_6\text{B})_2]^+[\text{PF}_6]^-$ (1) (Scheme 1)

A solution of $[\text{Fe}(\text{C}_5\text{H}_5)_2][\text{PF}_6]$ (330 mg, 1.00 mmol) in 50 ml of CH_2Cl_2 was added to one of $\text{Fe}(\text{C}_{15}\text{H}_{22}\text{N}_6\text{B})_2$ (650 mg, 1.00 mmol) in 50 ml of CH_2Cl_2 . A red solid separated immediately. The CH_2Cl_2 was removed on a rotary evaporator and the solid was washed with toluene to remove ferrocene. Recrystallisation from CH_2Cl_2 by slow evaporation of the solvent at room temperature gave dark red crystals of **1** (481 mg, 61%). Anal: Calcd. (Found) for $\text{C}_{30}\text{H}_{44}\text{B}_2\text{F}_6\text{FeN}_{12}$: C, 45.28 (45.30); H, 5.53 (5.59); N, 21.13 (21.11); Fe 7.04 (7.42)%.

2.3. Synthesis of $[\text{Fe}(\text{C}_{15}\text{H}_{22}\text{N}_6\text{B})_2]^+[\text{TCNQ}]^- \cdot \text{THF}$ (2)

A solution of $[\text{Fe}(\text{C}_{15}\text{H}_{22}\text{N}_6\text{B})_2]$ (100 mg, 0.15 mmol) in 20 ml of THF was added to one of TCNQ (30 mg, 0.147 mmol) in 5 ml of hot THF. The solution was concentrated to 10 ml and kept overnight at 4°C to yield dark blue crystals of **2** (72 mg, 52%). Anal. Calcd (Found) for $\text{C}_{46}\text{H}_{52}\text{B}_2\text{FeN}_{16}\text{O}$: C, 59.86 (59.90); H, 5.63 (5.88); N, 24.29 (24.69)%. Infrared (Nujol) $\nu(\text{C}\equiv\text{N}) = 2179, 2153 \text{ cm}^{-1}$.

2.4. Synthesis of $[\text{Fe}(\text{C}_{15}\text{H}_{22}\text{N}_6\text{B})_2]^+[\text{FeBr}_4]^-$ (3)

A solution of FeBr_3 (200 mg, 0.675 mmol) in 20 ml CH_2Cl_2 was added to a CH_2Cl_2 solution of $[\text{K}(\text{C}_{15}\text{H}_{22}\text{N}_6\text{B})]$ (295 g, 0.675 mmol) and the red mixture was stirred overnight under nitrogen then filtered. The filtrate was concentrated to 10 ml and diethyl ether was added dropwise to induce precipitation of fine red crystals of **3** (180 mg, 52%). Anal: Calcd (Found) for $\text{C}_{30}\text{H}_{44}\text{B}_2\text{BrFeN}_{12}$: C, 35.22 (35.52); H, 4.33 (4.35); N, 16.44 (15.98)%.

2.5. Crystal structure determinations for 1 and 2

Crystal data, data collection and processing parameters are given in Table 1. The procedure was as follows. A crystal was mounted in a Lindemann tube (0.7 mm) under nitrogen and sealed with a small flame. This was transferred to the goniometer head of an Enraf-Nonius CAD4 diffractometer. Unit cell parameters were calculated from the setting angles of 25 carefully centred reflections. Three reflections were chosen as intensity standards and were measured every

Table 2
Selected intramolecular distances for **1** (e.s.d's in parentheses)

Atoms	Distance / Å
Fe(1)–N(11)	1.960(3)
Fe(1)–N(21)	1.970(3)
Fe(1)–N(31)	1.962(3)
P(1)–F(1)	1.552(4)
P(1)–F(2)	1.556(5)
P(1)–F(3)	1.571(4)
N(11)–N(12)	1.372(4)
N(11)–C(15)	1.355(5)
N(12)–C(13)	1.349(5)
N(12)–B(1)	1.540(6)
N(21)–N(22)	1.374(5)
N(21)–C(25)	1.353(5)
N(22)–C(23)	1.351(5)
N(22)–B(1)	1.524(6)
N(31)–N(32)	1.380(4)
N(31)–C(35)	1.348(5)
N(32)–C(33)	1.330(5)
N(32)–B(1)	1.543(5)
C(13)–C(14)	1.370(7)
C(13)–C(16)	1.498(6)
C(14)–C(15)	1.393(6)
C(15)–C(17)	1.495(6)
C(23)–C(24)	1.394(7)
C(23)–C(26)	1.489(7)
C(24)–C(25)	1.392(6)
C(25)–C(27)	1.483(7)
C(33)–C(34)	1.391(6)
C(33)–C(36)	1.494(6)
C(34)–C(35)	1.395(6)
C(35)–C(37)	1.497(6)

3600 s of X-ray exposure time, and three orientation controls were measured every 250 reflections. The data were corrected for Lorentz and polarisation effects [13].

For both structures the heavy atom positions were revealed by direct methods. Subsequent Fourier difference syntheses revealed the positions of the other non-hydrogen atoms. Non-hydrogen atoms were refined with anisotropic thermal parameters by full-matrix least-squares procedures. The hydrogen atoms were fixed in geometrically idealised positions. The hydrogen atoms were given isotropic thermal parameters according to the atom to which they were attached (these were not refined). For **1** and **2** an empirical absorption correction using *DIFABS* [14] was applied. A Chebyshev weighting scheme [15] was applied and the data were corrected for the effects of anomalous dispersion and isotropic extinction (via an overall extinction parameter) [16] in the final stages of refinement. All crystallographic calculations were performed using the *CRYSTALS* suite [17] on a MicroVAX 3800 computer in the Chemical Crystallography Laboratory, Oxford. Neutral atom scattering factors were taken from the usual sources [18].

The atomic coordinates are listed in Tables 2 and 3. Complete lists of bond lengths additional material

available from and angles and tables of thermal parameters have been deposited with the Cambridge Crystallographic Data Centre.

3. Results and discussion

3.1. Synthesis and crystal structure of $[\text{Fe}(\text{C}_{15}\text{H}_{22}\text{N}_6\text{B}_2)]^+[\text{PF}_6]^-$ (1)

Compound **1** was synthesised by the addition of a solution of $[\text{Fe}(\text{C}_5\text{H}_5)_2]^+[\text{PF}_6]^-$ in CH_2Cl_2 to one of $[\text{Fe}(\text{C}_{15}\text{H}_{22}\text{N}_6\text{B}_2)]$ in CH_2Cl_2 . The resulting solid was washed with toluene and then recrystallised from CH_2Cl_2 to give a good yield of a red crystalline solid.

Table 3
Selected intramolecular angles for **1** (e.s.d.'s in parentheses)

Atoms	Angle /°	Atoms	Angle /°
N(11)–Fe(1)–N(11)	179.99	N(12)–N(11)–Fe(1)	118.2(2)
N(21)–Fe(1)–N(11)	89.6(1)	C(15)–N(11)–Fe(1)	135.1(3)
N(21)–Fe(1)–N(11)	90.4(1)	C(15)–N(11)–N(12)	106.7(3)
N(21)–Fe(1)–N(21)	179.99	C(13)–N(12)–N(11)	109.9(3)
N(31)–Fe(1)–N(11)	89.8(1)	B(1)–N(12)–N(11)	117.9(3)
N(31)–Fe(1)–N(11)	90.2(1)	B(1)–N(12)–C(13)	132.2(4)
N(31)–Fe(1)–N(21)	89.5(1)	N(22)–N(21)–Fe(1)	117.2(3)
N(31)–Fe(1)–N(21)	90.5(1)	C(25)–N(21)–Fe(1)	135.2(3)
N(31)–Fe(1)–N(31)	179.99	C(25)–N(21)–N(22)	107.6(3)
F(1)–P(1)–F(1)	179.99	C(23)–N(22)–N(21)	109.6(4)
F(2)–P(1)–F(1)	89.3(4)	B(1)–N(22)–N(21)	118.8(3)
F(2)–P(1)–F(1)	90.7(4)	B(1)–N(22)–C(23)	131.5(4)
F(2)–P(1)–F(2)	179.99	N(32)–N(31)–Fe(1)	117.8(2)
F(3)–P(1)–F(1)	89.8(3)	C(35)–N(31)–Fe(1)	135.4(3)
F(3)–P(1)–F(1)	90.2(3)	C(35)–N(31)–N(32)	106.7(3)
F(3)–P(1)–F(2)	88.4(3)	C(33)–N(32)–N(31)	110.0(3)
F(3)–P(1)–F(2)	91.6(3)	B(1)–N(32)–N(31)	117.8(3)
F(3)–P(1)–F(3)	179.99	B(1)–N(32)–C(33)	132.2(3)
C(14)–C(13)–N(12)	107.7(4)		
C(16)–C(13)–N(12)	123.4(4)		
C(16)–C(13)–C(14)	128.9(4)		
C(15)–C(14)–C(13)	107.0(4)		
C(14)–C(15)–N(11)	108.7(4)		
C(17)–C(15)–N(11)	124.2(4)		
C(17)–C(15)–C(14)	127.1(4)		
C(24)–C(23)–N(22)	107.4(4)		
C(26)–C(23)–N(22)	123.5(5)		
C(26)–C(23)–C(24)	129.1(4)		
C(25)–C(24)–C(23)	106.8(4)		
C(24)–C(25)–N(21)	108.6(4)		
C(27)–C(25)–N(21)	125.6(4)		
C(27)–C(25)–C(24)	125.8(4)		
C(34)–C(33)–N(32)	108.3(4)		
C(36)–C(33)–N(32)	122.4(4)		
C(36)–C(33)–C(34)	129.3(4)		
C(35)–C(34)–C(33)	105.8(4)		
C(34)–C(35)–N(31)	109.3(3)		
C(37)–C(35)–N(31)	125.6(4)		
C(37)–C(35)–C(34)	125.1(4)		
N(22)–B(1)–N(12)	108.5(3)		
N(32)–B(1)–N(12)	107.8(3)		
N(32)–B(1)–N(22)	107.6(3)		

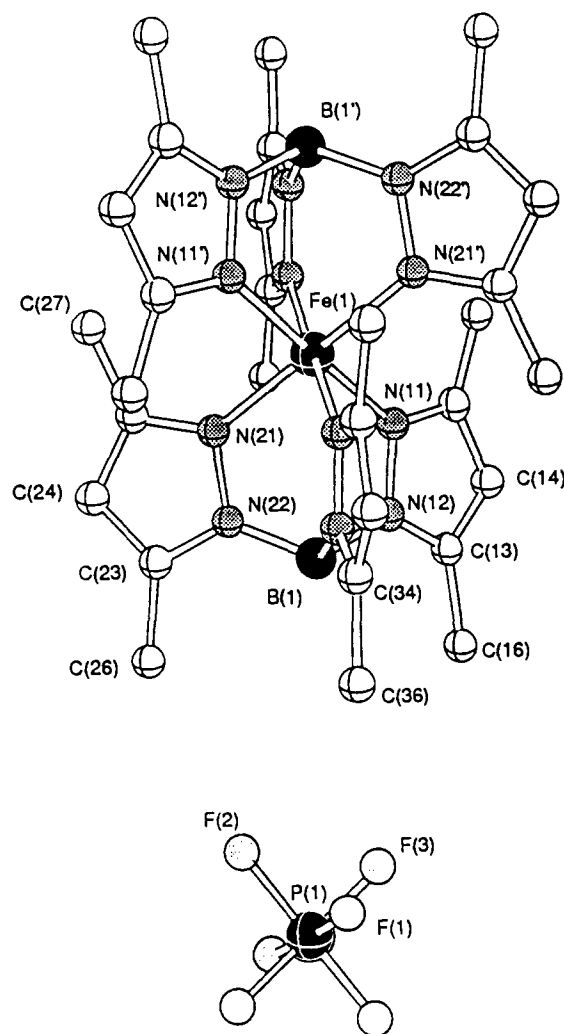


Fig. 1. Molecular Structure of **1** showing atomic labelling scheme, Atoms labeled (') are related by centre of inversion.

Compound **1** crystallises in the monoclinic space group $P2_1/a$. The molecular structure and atom labelling scheme is shown in Fig. 1. The structure determination reveals that both iron and phosphorus atoms are situated on crystallographic inversion sites (Fe $0, 1/2, 1/2$; P $1/2, 1/2, 0$) within the asymmetric unit. The coordination geometry around the Fe centre is almost perfectly octahedral with the Fe–N bond distances in the range 1.960(3)–1.970(3) Å, which are typical for low spin iron(III) complexes. The pyrazole rings are essentially planar. The mean N–N and B–N bond lengths are 1.375(3) and 1.536(3) Å, in close agreement with the values reported for other dimethylpyrazolyl borate complexes [9].

3.2. Synthesis and crystal structure of $[\text{Fe}(\text{C}_{15}\text{H}_{22}\text{N}_6\text{B}_2)]^+[\text{TCNQ}]^- \cdot \text{THF}$ (2)

Compound **2** was synthesised by addition of a solution of TCNQ in THF to one of $[\text{Fe}(\text{C}_{15}\text{H}_{22}\text{N}_6\text{B}_2)]$ in

Table 4
Selected intramolecular distances for **2** (e.s.d's in parentheses)

Atoms	Distance/Å	Atoms	Distance/Å
Fe(1)–N(1)	1.980(3)	C(11)–C(14)	1.499(5)
Fe(1)–N(1')	1.980(3)	C(12)–C(13)	1.394(5)
Fe(1)–N(3)	1.949(3)	C(13)–C(15)	1.500(5)
Fe(1)–N(3')	1.949(3)	C(31)–C(33)	1.410(5)
Fe(1)–N(5)	1.968(3)	C(32)–C(33)	1.415(6)
Fe(1)–N(5')	1.968(3)	C(33)–C(34)	1.419(5)
B(1)–N(2)	1.543(5)	C(34)–C(35)	1.409(5)
B(1)–N(4)	1.544(5)	C(34)–C(36)	1.401(5)
B(1)–N(6)	1.536(5)	C(35)–C(36')	1.438(5)
N(1)–N(2)	1.381(4)	C(41)–C(42)	1.521(9)
N(1)–C(3)	1.368(4)	C(41)–C(44)	1.22(3)
N(2)–C(1)	1.354(4)	C(41)–C(45)	1.524(8)
N(3)–N(4)	1.383(4)	C(42)–C(43)	1.540(9)
N(3)–C(8)	1.360(4)	C(42')–C(43')	1.67(3)
N(4)–C(6)	1.355(4)	C(43)–C(44)	1.49(1)
N(5)–N(6)	1.383(3)	C(44)–C(45)	1.486(9)
N(5)–C(13)	1.350(4)		
N(6)–C(11)	1.350(4)		
N(13)–C(32)	1.162(5)		
N(14)–C(31)	1.148(6)		
C(1)–C(2)	1.374(5)		
C(1)–C(4)	1.501(5)		
C(2)–C(3)	1.387(5)		
C(3)–C(5)	1.493(5)		
C(6)–C(7)	1.382(5)		
C(6)–C(9)	1.492(5)		
C(7)–C(8)	1.391(5)		
C(8)–C(10)	1.500(5)		

THF. After concentration the saturated solution was kept at 4°C to deposit blue crystals.

Compound **2** crystallises in the triclinic space group $P\bar{1}$. The molecular structure and atom labelling scheme is shown in Fig. 2. The important interatomic bond lengths and angles are given in Tables 3 and 4 respectively. The Fe atom (0,0,0), the centroid of the TCNQ anion and the THF were located on crystallographic inversion centres. The coordination environment of the iron atom is again essentially octahedral, with Fe–N bond lengths in the range 1.980(3)–1.949(2) Å. The pyrazole rings are again essentially planar. The observed bond lengths for the [TCNQ][−] anion are comparable with those found in similar complexes [10–12], with internal benzoid C–C bond lengths in the range 1.438(5)–1.401(5) Å, and C≡N bond lengths of 1.148(6) and 1.162(5) Å. The THF is disordered about a crystallographic inversion centre with each orientation at half occupancy; it was not possible to identify which ring atom was the oxygen of the THF molecule, so all atoms were set as carbon {C(41)–C(45) and C(41')–C(45')}.

We were particularly interested in examining the backing of anions and cations in **2** in order to look at any interatomic contacts closer than the sums of the van de Waals radius of the relevant atoms. Fig. 3 shows a packing diagram of **2** viewed along the crystallographic *a*-axis. The [TCNQ][−] anions lie in rows per-

pendicular to the crystallographic *bc*-plane, which are separated by parallel rows of [Fe(C₁₅H₂₂N₆B)₂]⁺ cations. Fig. 3 also shows the intermolecular separation of adjacent [TCNQ][−] ions. This side by side configuration does not lead to significant spin-spin exchange interactions between adjacent radical anions and cations (vide infra).

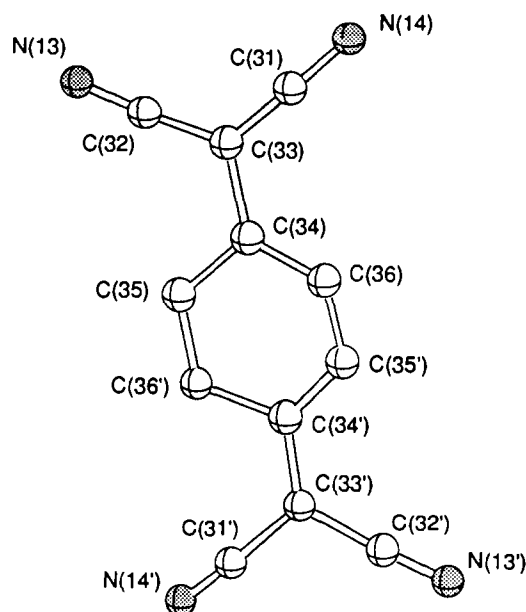
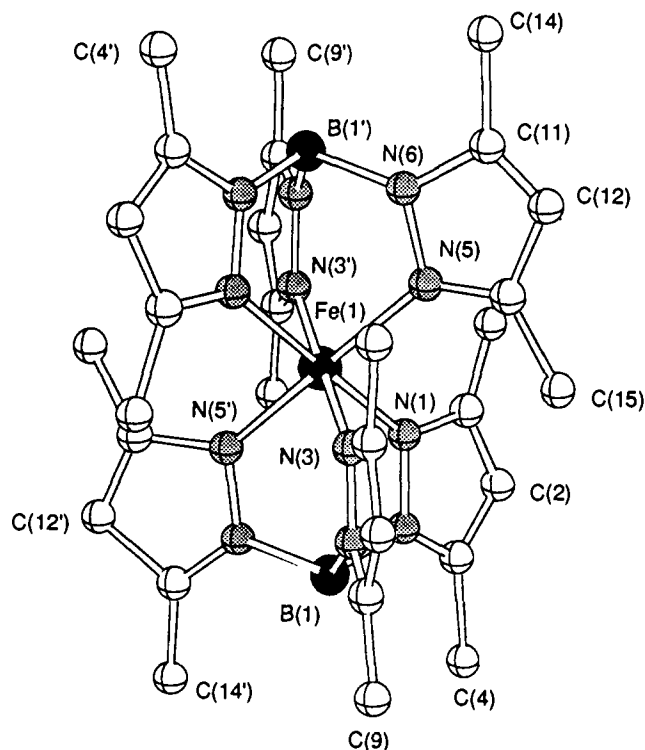


Fig. 2. Molecular structure of **2** showing atomic labelling scheme. Atoms denoted (') are related by crystallographic inversion centre. The disordered THF molecules have been omitted for clarity.

3.3. Synthesis of $[\text{Fe}(\text{C}_{15}\text{H}_{22}\text{N}_6\text{B})_2]^+[\text{FeBr}_4]^-$ (**3**)

Compound **3** was prepared by addition of a solution of FeBr_3 in CH_2Cl_2 one of $[\text{K}^+(\text{C}_{15}\text{H}_{22}\text{N}_6\text{B})^-]$ in CH_2Cl_2 . Dropwise addition of diethyl ether yielded red crystals of **3**.

3.4. Magnetic susceptibility measurements

Solid state magnetic susceptibility measurements were performed on compounds **1–3** in the temperature range 6–300 K. The magnetic susceptibilities of these compounds obey the Curie law $\chi_M = C/T$. The reciprocal susceptibilities of each compound as a function of temperature are shown in Fig. 4. For compound **1**, $\mu_{\text{eff}} = 1.68 \mu_B \pm 0.05$ (6–265 K), which is consistent with the existence of a single $S = 1/2$ spin, that of the $[\text{Fe}(\text{C}_{15}\text{H}_{22}\text{N}_6\text{B})_2]^+$ ion. For compound **2** $\mu_{\text{eff}} = 2.55 \mu_B \pm 0.2$ (6–300 K), which is consistent with the two non-interacting $S = 1/2$ spins of the $[\text{Fe}(\text{C}_{15}\text{H}_{22}\text{N}_6\text{B})_2]^+$ and $[\text{TCNQ}]^-$ ions respectively. For compound **3** $\mu_{\text{eff}} = 5.39 \mu_B \pm 0.05$ (6–300 K), which is consistent with two non-interacting spins, the $S = 1/2$ $[\text{Fe}(\text{C}_{15}\text{H}_{22}\text{N}_6\text{B})_2]^+$ and $S = 5/2$ $[\text{FeBr}_4]^-$. The effective moment for two non-interacting spins, using the spin-only formula, is given by the expression:

$$\mu_{\text{eff}}^2 = g_{\text{cation}}^2 [S(S+1)] + g_{\text{anion}}^2 [S(S+1)]$$

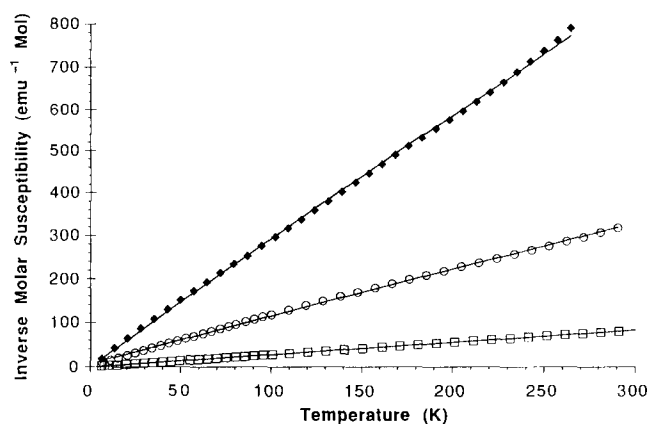


Fig. 4. Plot of inverse molar magnetic susceptibility (χ_M^{-1}) versus temperature (T) for compounds (**1** \blacklozenge ; **2** \circ ; **3** \square).

Compound **3** has an effective moment slightly higher than the predicted spin-only value ($2.44 \mu_B$) and compound **3** has an effective moment slightly lower than the predicted spin-only value ($6.18 \mu_B$). The absence of π -electron density on the pyrazolyl borate ligand prevents the degree of intermolecular interaction between the $[\text{Fe}(\text{C}_{15}\text{H}_{22}\text{N}_6\text{B})_2]^+$ cations and the $[\text{TCNQ}]^-$ anions that has been seen in the charge-transfer salt $[\text{Fe}(\text{C}_5\text{Me}_5)_2][\text{TCNQ}]$, and results in the former displaying simple paramagnetic behaviour over the temperature range studied.

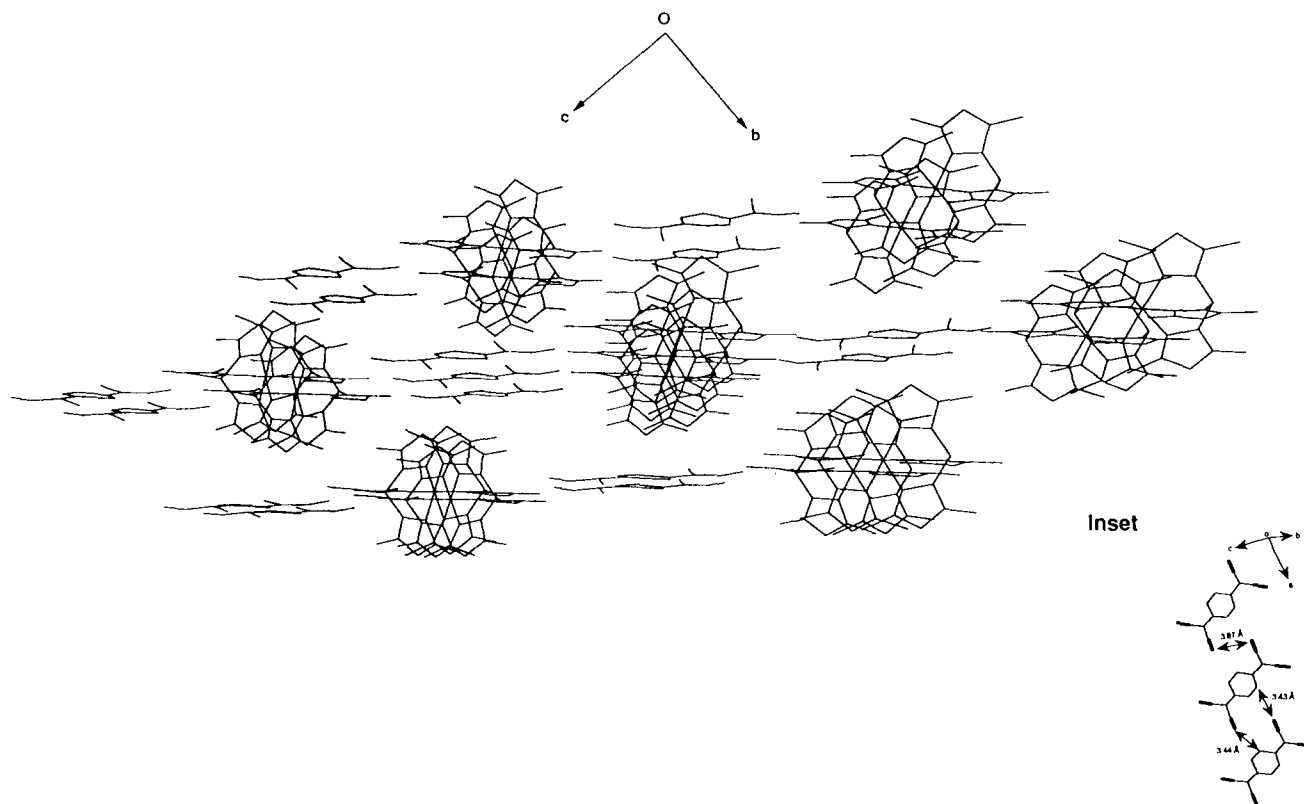


Fig. 3. Packing diagram for **2** viewed down the crystallographic a -axis. Inset shows the inter-anion separations along a sheet of TCNQ molecules. The disordered THF molecules have been omitted for clarity.

Table 5
Selected intramolecular angles for 2 (e.s.d's in parentheses)

Atoms	Angle/°	Atoms	Angle/°
N(1)–Fe(1)–N(1')	179.99	N(5)–C(13)–C(15)	124.4(3)
N(1)–Fe(1)–N(3)	89.8(1)	C(12)–C(13)–C(15)	126.8(3)
N(1)–Fe(1)–N(3)	90.2(1)	N(14)–C(31)–C(33)	177.1(5)
N(1)–Fe(1)–N(3')	90.2(1)	N(13)–C(32)–C(33)	178.1(4)
N(1)–Fe(1)–N(3)	89.8(1)	C(31)–C(33)–C(32)	117.0(3)
N(3)–Fe(1)–N(3')	179.99	C(31)–C(33)–C(34)	120.7(4)
N(1)–Fe(1)–N(5)	89.6(1)	C(32)–C(33)–C(34)	122.0(3)
N(1)–Fe(1)–N(5')	90.4(1)	C(33)–C(34)–C(35)	119.5(3)
N(3)–Fe(1)–N(5)	90.0(1)	C(33)–C(34)–C(36)	121.0(3)
N(3)–Fe(1)–N(5')	90.0(1)	C(35)–C(34)–C(36)	119.5(3)
N(1)–Fe(1)–N(5)	90.4(1)	C(34)–C(35)–C(36)	119.4(3)
N(1)–Fe(1)–N(5')	89.6(1)	C(34)–C(36)–C(35)	121.1(3)
N(3)–Fe(1)–N(5)	90.0(1)	C(42)–C(41)–C(43)	102.0(46)
N(3')–Fe(1)–N(5')	90.0(1)	C(43)–C(41)–C(44)	120.8(57)
N(5)–Fe(1)–N(5')	179.99	C(42)–C(41)–C(45)	102.2(6)
N(2)–B(1)–N(4)	108.2(3)	C(44)–C(41)–C(45)	121.6(20)
N(2)–B(1)–N(6)	106.7(3)	C(41)–C(42)–C(43)	100.4(7)
N(4)–B(1)–N(6)	107.2(3)	C(43)–C(42)–C(43)	85.6(12)
Fe(1)–N(1)–N(2)	118.2(2)	C(43)–C(42)–C(44)	114.9(20)
Fe(1)–N(1)–C(3)	135.6(2)	C(41)–C(42)–C(45)	134.5(27)
N(2)–N(1)–C(3)	106.2(3)	C(43)–C(42)–C(45)	121.4(33)
B(1)–N(2)–N(1)	118.2(2)	C(44)–C(42)–C(45)	115.4(32)
B(1)–N(2)–C(1)	131.6(3)	C(41)–C(43)–C(42)	155.7(45)
N(1)–N(2)–C(1)	110.1(3)	C(42)–C(43)–C(42)	94.4(12)
Fe(1)–N(3)–N(4)	118.2(2)	C(42)–C(43)–C(44)	112.0(9)
Fe(1)–N(3)–C(8)	135.2(2)	C(41)–C(43)–C(45)	178.5(81)
N(4)–N(3)–C(8)	106.6(3)	C(42)–C(43)–C(45)	117.2(23)
B(1)–N(4)–N(3)	118.7(2)	C(44)–C(43)–C(45)	136.7(18)
B(1)–N(4)–C(6)	131.4(3)	C(41)–C(44)–C(42)	85.1(19)
N(3)–N(4)–C(6)	109.9(3)	C(42)–C(44)–C(43)	80.9(19)
Fe(1)–N(5)–N(6)	117.7(2)	C(41)–C(44)–C(45)	101.2(15)
Fe(1)–N(5)–C(13)	135.2(2)	C(43)–C(44)–C(45)	91.9(8)
N(6)–N(5)–C(13)	107.1(2)	C(41)–C(45)–C(42)	115.6(28)
B(1)–N(6)–N(5)	119.0(2)	C(42)–C(45)–C(43)	115.4(34)
B(1)–N(6)–C(11)	131.7(3)	C(41)–C(45)–C(44)	115.0(7)
N(5)–N(6)–C(11)	109.4(3)	C(43)–C(45)–C(44)	115.1(20)
N(2)–C(1)–C(2)	107.4(3)		
N(2)–C(1)–C(4)	123.2(3)		
C(2)–C(1)–C(4)	129.4(3)		
C(1)–C(2)–C(3)	107.6(3)		
N(1)–C(3)–C(2)	108.7(3)		
N(1)–C(3)–C(5)	124.4(3)		
C(2)–C(3)–C(5)	126.9(3)		
N(4)–C(6)–C(7)	107.3(3)		
N(4)–C(6)–C(9)	124.0(3)		
C(7)–C(6)–C(9)	128.6(3)		
C(6)–C(7)–C(8)	107.2(3)		
N(3)–C(8)–C(7)	108.9(3)		
N(3)–C(8)–C(10)	124.3(3)		
C(7)–C(8)–C(10)	126.7(3)		
N(6)–C(11)–C(12)	107.9(3)		
N(6)–C(11)–C(14)	122.3(3)		
C(12)–C(11)–C(14)	129.8(3)		
C(11)–C(12)–C(13)	106.8(3)		
N(5)–C(13)–C(12)	108.9(3)		
N(5)–C(13)–C(15)	124.4(3)		

4. Summary

Salts containing the bis[hydrotris(1-pyrazolyl)borate]iron(III) cation have been synthesised by a variety of

routes and characterised using single crystal X-ray diffraction. The magnetic studies on these compounds indicate a low spin configuration for the iron(III) complex over the temperature range 6–300 K; there is no evidence for any spin-spin interactions in these salts at low temperature. This is in agreement with the X-ray data which showed no anion-anion or anion-cation separations closer than the sum of the van der Waals radii of the relevant atoms. In addition the d^5 Fe^{III} metal centres in all the salts were in the low spin ($S = 1/2$) configuration and in contrast to the neutral bis[hydrotris(3,5-dimethyl-1-pyrazolyl)borate]iron(II) complex showed no evidence for a high spin-low spin transition.

Acknowledgement

We thank the SERC for financial support.

References

- [1] J.S. Miller, J.C. Calabrese, H. Rommelmann, S.R. Chittipeddi, J.H. Zhang, W.M. Reiff and A.J. Epstein, *J. Am. Chem. Soc.*, **109** (1987) 769.
- [2] J.S. Miller, R.S. McLean, C. Vazquez, J.C. Calabrese, F. Zuo and A.J. Epstein, *J. Mater. Chem.*, **3** (1993) 215.
- [3] G.T. Yee, J.M. Manriquez, D.A. Dixon, R.S. McLean, D.M. Groski, R.B. Flippen, K.S. Narayan, A.J. Epstein and J.S. Miller, *Adv. Mater.*, **3** (1991) 309.
- [4] A.H. Cowley, C.J. Carrano, R.L. Geerts, R.A. Jones and C.M. Nunn, *Angew. Chem., Int. Ed. Engl.*, **27** (1988) 277.
- [5] J.A. McCleverty, *Inorg. Chim. Acta.*, **62** (1982) 647.
- [6] S. Trofimenko, *J. Am. Chem. Soc.*, **89** (1967) 6288.
- [7] J.P. Jesson, S. Trofimenko and D.R. Eaton, *J. Am. Chem. Soc.*, **89** (1967) 3158.
- [8] J.P. Jesson, J.F. Weiher and S. Trofimenko, *J. Chem. Phys.*, **48** (1968) 2058.
- [9] M.R. Churchill, K. Gold and J.C.E. Maw, *Inorg. Chem.*, **9** (1970) 1597.
- [10] V. Murphy and D. O'Hare, *Inorg. Chem.*, **33** (1994) 1833.
- [11] J.S. Miller, J.H. Zhang, W.M. Reiff, D.A. Dixon, L.D. Preston, J.A.H. Reis, E. Gebert, M. Extine, J. Troup, A.J. Epstein and M.D. Ward, *J. Phys. Chem.*, **91** (1987) 4244.
- [12] J.S. Miller, D.T. Glatzhofer, D.M. O'Hare, W.M. Reiff, A. Chakraborty and A.J. Epstein, *J. Am. Chem. Soc.*, **28** (1989) 2930.
- [13] A.C.T. North, D.C. Phillips, and F.S. Mathews, *Acta Crystallogr.*, **A24** (1968) 351.
- [14] N. Walker and D. Stuart, *Acta Crystallogr.*, **A24** (1968) 351.
- [15] J.S. Rollet, *Computing Methods in Crystallography*, Pergamon, Oxford, 1965.
- [16] A.C. Larsen, *Acta Crystallogr.*, **23** (1967) 664.
- [17] D.J. Watkin, J.R. Carruthers and P.W. Betteridge, *CRYSTALS User Guide*, Chemical Crystallography Laboratory, University of Oxford, 1985.
- [18] *International Tables for X-ray Crystallography*, Kynoch, Birmingham, Vol. 4, 1974, 9.